Biocatalysis and Agricultural Biotechnology 20 (2019) 101237

Contents lists available at ScienceDirect

Biocatalysis and Agricultural Biotechnology

journal homepage: www.elsevier.com/locate/bab

Medicinal impact of microalgae collected from high rate algal ponds; phytochemical and pharmacological studies of microalgae and its application in medicated bandages

Rehab A. Hussein[a], Abeer A.A. Salama[b], Mehrez E. El Naggar[c,*], Gamila H. Ali[d]

[a] Pharmacognosy Department, National Research Centre, Giza, Egypt
[b] Pharmacology Department, National Research Centre, Giza, Egypt
[c] Textile Research Division, National Research Centre, Giza, Egypt
[d] Water Pollution Research Department, National Research Centre, Giza, Egypt

ARTICLE INFO

Keywords:
High rate algal ponds
Microalgae
Phytochemical study
Antidiabetic activity
Wound healing
Medicated bandages

ABSTRACT

In the course of maximizing the utilization of natural resources, microalgal communities growing in high rate algal ponds are being investigated for possible pharmacological and medicinal values. An algal community predominated by *Microcystis aeruginosa* was phytochemically studied using Liquid chromatography with Photodiode array detector coupled with electron spary ionization mass spectroscopy (LC-DAD/ESI-MS). A pharmacological screening including antioxidant, anti-inflammatory, anti-diabetic and cytotoxic actions was conducted. The application of *Microcystis aeruginosa* predominant algal extract in formulating medicated bandages to aid healing of diabetic wounds was further evaluated. The phytochemical investigation of the algal extract led to the separation and identification of hydroxypheophytin-a, astaxanthin and phytoene in the algal extract which showed marked antioxidant and anti-inflammatory activities at 500 mg/kg dose level. At a dose of 200 and 400 mg/kg, it significantly diminished glucose levels in diabetic rats' sera in a dose-dependent manner. Marked decline in serum nitric oxide and catalase values was detected along with a significant increase in serum insulin, glucose transporter 2 and cluster of differentiation 4 levels. The obtained results indicated that the use of the algal based medicated bandages on wounds induced in diabetic rats showed progressive healing as compared to untreated rats. A considerable decrease in serum tumor necrosis factor-α accompanied by the increase in serum collagen-I was observed. The histopathological inspection of rats' skin ascertained the improvement in skin condition.

1. Introduction

Microalgae are important biological resources that possess a multitude of physiological, biochemical and molecular strategies to cope with stress; they produce several active phyto-constituents. These active compounds vary in their structures including fatty acids, polysaccharides, phycocyanins, carotenoids, enzymes and phenolic compounds (Singh et al., 2013). The isolated compounds show an array of pharmacological activities, including anticancer, antiviral, antioxidant, hepatoprotective, cardioprotective and immunomodulatory effects (El-Baz et al., 2018). Of the various groups of microalgae, the blue-green algae seem to feature most prominently as sources of bioactive compounds. Phycotoxins were proven to exert cytotoxic, antitumor, antibiotic, antifungal, immunosuppressant and neurotoxic potencies. A number of protease inhibitors were isolated from blue-green algae *viz*, cyclic or linear peptides and depsipeptides, which have potential applications in medicine for treatment of diseases such as strokes, coronary artery occlusions and pulmonary emphysema (Assunção et al., 2017). Aeruginosins isolated from *Microcystis aeruginosa* have shown inhibitory activity against thrombin, plasmin and trypsin (Murakami et al., 1995; Posadas et al., 2013). Depsipeptides as micropeptin, microcystilide, cyanopeptolin, oscillapeptin and nostocyclin also showed inhibitory effects on proteases as trypsin, plasmin, thrombin and chymotrypsin (Mazur-Marzec et al., 2018).

Microalgae are also potential sources of antiviral compounds. A novel compound from blue-green algae, cyanovirin-N has revealed potent virucidal agent against HIV, which blocks the interaction of the viral glycoprotein gp120 with CD4 (Tsai et al., 2004). The sulfated polysaccharide calcium spirulan isolated from *Spirulina platensis* showed antiviral efficacy against Herpes simplex, human

* Corresponding author.
E-mail addresses: Mehrez_chem@yahoo.com, mehrezeelnaggar@gmail.com (M.E. El Naggar).

https://doi.org/10.1016/j.bcab.2019.101237
Received 27 May 2019; Received in revised form 23 June 2019; Accepted 4 July 2019
Available online 05 July 2019
1878-8181/

cytomegaloviruses and measles virus (HAYASHI et al., 1996).

Algal-prokaryotic wastewater treatment provides added benefit of reduced expenses, energy supply and reduced pollutants emissions from power plants. The application of algae waste stabilization ponds (WSPs) was first introduced in 1950s (Oswald and Gotass, 1957). More recently, engineered algae-based wastewater treatment systems have been developed to reduce the footprint and improve nutrient removal efficiency and effluent specifications, namely high rate algal ponds (HRAPs), algal-prokaryotic bio-film reactors as well as enhanced algal-prokaryotic systems (EAPS) (Gross et al., 2015). These systems basically utilize algae for nutrient assimilation and the production of DO which is responsible for the degradation of organic matter and nitrification. Algae also act on the improvement of biomass settling ability, the mitigation of CO_2 and the increase of pH value which enhances the vaporization of ammonia and phosphate precipitation (Craggs et al., 2011). The bio-sorption activity of marine algae biomasses has been investigated for their the effective removal of potentially toxic elements from aqueous media (Bilal et al., 2018). HRAPs have been proven to be very effective for the production of bioenergy (e.g. biofuels), nutrients (e.g. biofertilizers) and algal bioactive compounds (e.g. pigments, lipids) from wastewater (Arashiro et al., 2019). The smaller footprint of HRAP systems coupled with the benefit of production of valuable products (e. g. biofuels, bioplastics) from microalgae feedstock makes them more attractive over WPS.

In sight of the above data, there is a large potential of discovering new drug leads from microalgae obtained from high rate algal ponds. The current study object to screen various pharmacological effects of microalgae collected from high rate algal pond; acute lethal toxicity, antioxidant, anti-inflammatory, anti-cancer and anti-diabetic effects and to identify its phytochemical constituents using LC-DAD/ESI-MS. Additionally, the application of the algal extract on medical bandages was evaluated for its efficacy to aid healing of diabetic wounds.

2. Materials and methods

2.1. Materials

2.1.1. High rate algal pond system (pilot scale system)

Race way-type pond (High Rate Algal Pond, HRAP) made of glass-fibre reinforced plastics (GRP) material, with 6.5 m^3 capacity without connection or separation. Its dimensions are (7m length × 3m width × 40 cm depth) and the effective wastewater depth is 0.3 m. The wastewater moves in the pond by an electric fan (paddle wheel) attached to the pond with dimensions of 140 cm width and 50 cm diameter and have 12 paddle with 70 cm width and made from Stainless Steel material. The fan connected to electric motor and speed controlling (5–15 round) to give a flow velocity of 0.2 m/s. The HRAP was constructed and installed in Zenin wastewater treatment plant- Giza Company for Water and Wastewater- Egypt (Fig. 1).

Algal biomass collected from high rate algal pond (1m^3) are harvested biweekly and precipitated by cationic starch (El-Naggar et al., 2018). The collected biomass was dried (using sun drier), grinded to fine particles (0.1 mm).

All animals used in the pharmacological studies were hosted in standard cages, under specific pathogen-free conditions in facilities maintained at controlled room temperature (21–24 °C) with a 40–60% relative humidity and under normal dark–light cycles. The animals were allowed to rat chow diet and water *ad libitum*. They were accustomed for a period of two weeks before the initiation of the experiments. All experimental procedures involving animal handling were granted approval by the Animal Care Committee of the National Research Centre according to “Principles of laboratory animal care” and specific national laws.

2.2. Methods

2.2.1. Identification of algal community contained in the high rate algal pond

Along one year, algal biomass was collected twice a week and subsamples were allocated into glass Sedgwick-Rafter cells and investigated using OLYMPUS CX41® microscope. Species constituting the samples were defined pointing out the dominant species in a semi-quantitative manner. Algal identification has been done in accordance with the chief references used in phytoplankton identification (Streble and Krauter, 2006).

2.2.2. Preparation of Microcystis aeruginosa predominant algal extract (MAPE)

The dried biomass collected from high rate algal pond in the period of *Microcystis aerigunosa* predominance was grinded thoroughly for cell wall disruption. The algal extract was prepared by solvent extraction using methanol: chloroform 50:50 till exhaustion. It was then dried in a rotary-evaporator under reduced pressure, at a temperature less than 40 °C till entirely dry. The dried fraction was kept in dark containers in dry and cold conditions (4 °C) for further analysis Hussein et al., 2018).

2.2.3. Preparation of cotton bandage fabrics treated with different concentrations of MAPE

The samples of scoured, bleached cotton bandage fabrics were immersed in pad baths containing 200 mg and 400 mg of algal extract solution for 15 min. The samples of cotton bandage fabrics were padded in the previously prepared solution in two dips and nips, and then squeezed to a wet pick-up of 100%. The Padded fabrics were dried at 80 °C for 5 min and then cured at120 °C for 3 min. Treated fabrics were rinsed with hot water then with cold water and finally dried at room temperature. The color of bleached cotton bandage fabric was turned from white to greenish color confirming the deposition of algal extract on the surface of bleached cotton bandage fabrics(El-Naggar et al., 2018; Elshaarawy et al., 2019).

2.2.4. Pharmacological evaluation of MAPE and MAPE loaded cotton bandage fabrics

2.2.4.1. Acute toxicity study. Twenty Swiss mice of 20–30 g body weight were used for the acute toxicity assay. The dried MAPE was suspended in distilled water and orally administered to rats in gradually increasing doses up to 5 g/kg. A control group receiving equivalent volumes of distilled water was used. Mortality percentage was recorded 24 h later (Desoukey et al., 2016). Observation of rats for 14 days, for any changes in the skin and fur, respiratory, circulatory, autonomic, somato-motor activity, salivation, diarrhoea and behaviour pattern. Particular observation was given for central nervous system alteration as manifested by tremors, convulsions, lethargy, sleep, and coma (El-Naggar et al., 2019).

2.2.4.2. Antioxidant activity (DPPH radical scavenging activity). The DPPH assay was performed according to Desoukey et al. (2016) (Desoukey et al., 2016). A solution of 2,2-Diphenyl-1-picrylhydrazyl radical (DPPH, Sigma, USA) in methanol (0.004% solution) was prepared and stored in dark until use. Preparation of the tested fractions at different concentrations was done in methanol. In a 96-well plate, addition of 20 µl of each concentration to 180 µl DPPH solution was carried out. Negative controls were done to correct for colored fractions. The produced reaction solutions were vortexed and incubated at room temperature for 30 min. UV-visible absorbencies of reaction solutions were recorded spectrophotometerically at a wavelength of 520 nm against methanol (blank) and DPPH solution without addition of extract was used as control. Ascorbic acid was used as reference standard. DPPH radical scavenging power was calculated according to the following equation:

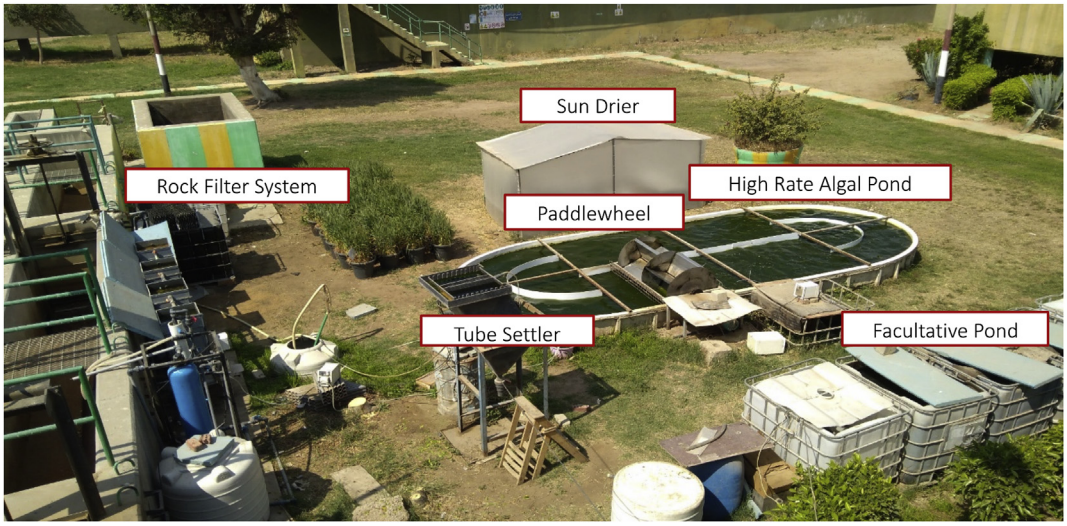

Fig. 1. Illustration the high rate algal pond (HRAP) pilot scale.

$$\textit{Scavenging activity}\ (\%)\frac{A0 - A1}{A0} \times 100$$

where A_0 is the absorbance of the control and A_1 is the absorbance of the algal extract or reference standard. EC_{50} values; algal dose exerting 50% scavenging activity, were estimated from the graph of percentage of inhibition plotted against the concentrations of the extract; using GraphPad Prism Software version 5.0.

2.2.4.3. Anti-inflammatory activity (Carrageenan induced paw edema). Thirty adult male Wister albino rats (7-8-weeks old, weighing 130–180 g) were used for anti-inflammatory assay. Paw swelling was induced by sub-plantar infusion of 100 µl of 1% sterile lambda carrageenan (Sigma, USA) suspension in saline into the right hind paw (Fehrenbacher et al., 2012). Inflammation was estimated through the determination of the edema extent as percentage of change from control by measuring hind footpad thickness using a micrometer caliber before carrageenan injection (basal) and 1- 4 h after carrageenan injection (Obukowicz et al., 1998). Rats were sorted into 3 groups, ten rats each, receiving saline (0.2 ml/rat), indomethacin (Epico, Egypt Int. pharmaceutical Industries Co., ARE under license of MERCK Co. Inc-Rahaway, NJ, USA) (25 mg/kg) and algal extract (500 mg/kg), respectively. Indomethacin and the treatment were given orally 60 min before the injection of carrageenan injection.

2.2.4.4. Cytotoxic activity on human cancer cell lines. Cell viability was measured colorimetrically using MTT (3-(4,5-dimethylthiazol-2-yl)-2,5-diphenyl tetrazolium bromide) (). All procedures were held under sterile conditions in Laminar flow cabinet bio-safety class II level (Baker, SG403INT, Sanford, ME, USA). Cells were suspended in RPMI 1640 media for He-PG2- MCF-7 and HCT-116 cells and DMEM media for A-549 and PC-3 cells. 1% antibiotic-antimycotic mixture (10,000U/ml Potassium Penicillin, 10,000µg/ml Streptomycin Sulphate and 25µg/ml Amphotericin B) and 1% L-glutamine were added to the culture media which is kept at 37 °C and 5% CO_2. Cells were seeded at a concentration of $10x10^3$ cells per well in 96-well microtiter plastic plates using fresh complete growth medium and incubated at 37 °C for 24 h under 5% CO_2 in a water-jacketed CO_2 incubator (Sheldon, TC2323, Cornelius, OR, USA). Fresh media was added and cells were incubated after the addition of the algal extract at different concentrations (100-50-25-12.5-6.25-3.125-0.78 and 1.56 µg/ml) and a negative control was left without treatment. After 48 h of incubation, media was stripped off, MTT salt (2.5 µg/ml) was added 40 µl/well and the plates were incubated for further 4 h at 37 °C and 5% CO_2. The color reaction is terminated using 10% Sodium dodecyl sulphate (SDS) in deionized water. A positive control cytotoxic natural agent was applied under the same conditions. Absorbance was then measured using a microplate multi-well reader (Bio-Rad Laboratories Inc., model 3350, Hercules, California, USA) at wavelength 595 nm and a reference wavelength of 620 nm. Statistical data were analyzed using independent *t*-test by SPSS 11 program between treatments and negative control. DMSO used as vehicle for dissolution of algal extract and its final concentration was less than 0.2%. The percentage of change in viability was calculated according to the equation:

$$\textbf{Viability}\ \textit{change}\ (\%) = \left(\frac{\textit{Absorbance of extract}}{\textit{Absorbance of negative control}} - 1\right) \times 100$$

A probit analysis was carried for IC_{50} and IC_{90} determination using SPSS 11 program.

2.2.4.5. Anti-diabetic effect (Streptozotacin-induced diabetes in rats). Albino Wistar rats of either sex weighing 150–250 g were used for anti-diabetic assay. Type I diabetes was induced by a single intraperitoneal injection of STZ (Sigma Aldrich Chemical Co., USA) (50 mg/kg) dissoluted in 0.1M citrate buffer (sodium citrate was obtained from Sigma Aldrich Chemical Co., USA) (pH 4.5) (Khalaf et al., 2012). The rats were sorted into five groups, where group 1 served as negative control; rats were treated with equivalent volume of citrate buffer without STZ for 1 week. Diabetes was confirmed after 48 h post STZ injection by estimating blood glucose level in blood samples withdrawn from the tail vein (One Touch SureStep Meter, LifeScan, Calif, USA). After diabetes was confirmed (> 200 mg/ml), rats were assigned randomly into four groups: Group 2 served as positive control (STZ-induced diabetic rats). Group 3 Diabetic rats received glimepiride (Aventis,Co., Egypt) (0.5 mg/kg; p.o.) (Salama and Yassen, 2017; Aly and Ali, 2016) for 1 week. Groups 4 and 5 diabetic rats received MAPE (200 mg and 400 mg/kg) for 1 week.

Biochemical analysis: Blood samples were drawn after overnight fast from retro-orbital venous plexus after 1 week then the blood was centrifuged (3000 rpm for 15 min) to get serum for measuring serum levels of glucose. Uchiyama and Mihara's method (1978) was adopted for the determination of malondialdhyde (MDA) as indication of lipid peroxidation (LPO) (Mihara and Uchiyama, 1978). Reduced glutathione (GSH) was determined according to Moron et al. (1979) (Moron et al., 1979); nitric oxide (NO) according to Miranda et al. (2001) (Miranda et al., 2001) and catalase (CAT) activity according to Aebi (1984) (Aebi, 1984) In addition insulin, glucose transporter 2 (GLUT2) and cluster of differentiation 4 (CD4) were estimated using SinoGeneClon Biotech Co., Ltd.

Table 1
Time course of the effect of pre-treatment with MAPE on paw edema thickness induced by sub-plantar injection of 1% carrageenan.

Time	Paw edema thickness (cm)				
	0	1 h	2h	3h	4h
Carrageenan	0.36 ± 0.01	0.62 ± 0.02	0.69 ± 0.02	0.72 ± 0.02	0.69 ± 0.01
Indomethacin	0.42 ± 0.03	0.53 ± 0.02*	0.59 ± 0.02*	0.54 ± 0.02*	0.52 ± 0.03*
500 mg/kg MAPE	0.35 ± 0.01	0.47 ± 0.01*	0.48 ± 0.01*	0.49 ± 0.01*	0.46 ± 0.01*

* Vs carrageenan control value at respective time point at $P < 0.05$.

Table 2
Cytotoxic activity of MAPE at 100 ppm concentration.

	MAPE (100 ppm)
HCT116 [Colon cell line]	**0%**
A549 [Lung carcinoma cell line]	**10%**
HePG 2 [Human hepatocellular carcinoma cell line]	**81.1%**
MCF7 [Human Caucasian breast adenocarcinoma]	**64.3%**
PC3 [Prostate cancer cell line]	**100%**

Histopathological investigation of pancreatic tissue: By the end of the experiment; animals were sacrificed. Pancreas (splenic part), and kidneys were excised from sacrificed animals. Organ tissues were fixed in 10% buffered formalin, processed through increasing concenterations of alcohol, cleared in xylene and prepared into paraffin blocks. Serial sections 5 µm thick were prepared from each block and stained using haematoxylin and eosin for routine histopathologic study.

2.2.4.6. Physical and biochemical analysis of MAPE loaded cotton bandage fabric

2.2.4.6.1. Physical analysis of MAPE loaded cotton bandage fabric. The surface morphology of the untreated and cotton bandage fabrics treated with MAPE solution was examined using the JSM-6390 Scanning electron microscope (SEM).

2.2.4.6.2. Evaluation of wound healing effect. **Induction of diabetes:** Diabetes was induced by single intraperitoneal injection of STZ (50 mg/kg) dissolved in 0.1 M citrate buffer (pH 4.5). The animals were allowed to drink 5% glucose solution overnight to overcome the drug induced hypoglycemia. 48 h after injection of STZ, fasting plasma blood glucose was estimated. Animals with plasma glucose of > 200 mg/dl were selected.

Wound excision: The dorsal skin of the rats was shaved with an electric razor 1 day prior to the experiment. On the day of experiment, rats were divided into 4 groups (n = 8 per group). Group I served as a negative control (non-wounded) and the other three groups were subjected to thiopental anesthesia and subjected to wound excision. Full-thickness skin excision round wounds of 5 mm in diameter were created using a sterile biopsy punch needle (No. 5, Ribbel international Ltd., India). Wound healing was assessed by measuring the reduction of the wound length after 7 day injury (Asfour et al., 2017).

Biochemical analysis: Wounded tissues of rats from different groups were collected after ten days post-wounding and 20% (w/v) homogenate was prepared in phosphate buffer (50 mM, pH 7.4) with homogenizer (Medical instruments, MPW-120, Poland). The crude homogenate was centrifuged at 1000 rpm at 4 °C for 10 min (Laborzentrifugen, 2k15, Sigma, Germany) to pellet down nuclei as well as other cell debris. The resultant supernatant was subjected to several biochemical analyses as TNF-α and collagen I. Data are expressed as mean ± S.E. Data analysis was done using one way analysis of variance (ANOVA) followed by Tukey test for multiple comparisons. Difference was considered significant when p is less than 0.05. SPSS (version 11) program was used to carry out these statistical tests.

Histopathological examination: A biopsy sample was stored from each group, rinsed with distilled water, and then dehydrated alcohols with increasing concentrations (methanol, ethanol and absolute ethanol). Specimens were cleared in xylene and immersed in paraffin in hot air oven at 56 °C for 24 h. Paraffin bees wax tissue blocks were excised by a microtome into tissue sections 5 µm thick. Sections were then applied on glass slides and stained with haematoxylin and eosin stain after removal of paraffin for inspection using optical microscope, (Leica Qwin 500 Image Analyzer (LEICA Imaging Systems Ltd, Cambridge, England) composed of Leica DM-LB microscope with JVC color video camera attached to a computer system Leica Q 500IW). Wounded tissue samples of all the investigated groups were blindly examined.

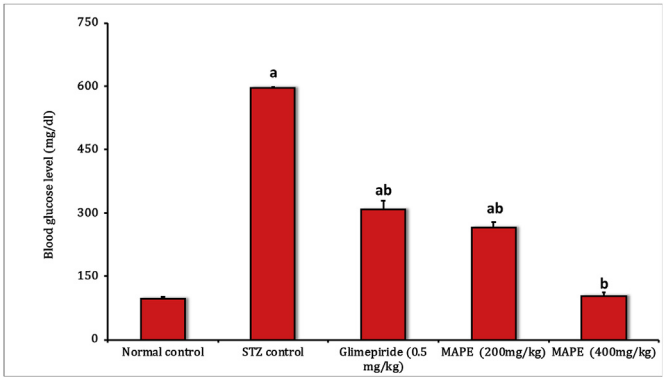

Fig. 2. Effect of MAPE on blood glucose level; Data were expressed as mean ± SE. Statistical analysis was carried out by one-way ANOVA followed by Tukey HSD test for multiple comparisons. [a] Significantly different from normal control at $P < 0.05$. [b] Significantly different from STZ control at $P < 0.05$.

2.2.5. Phytochemical analysis of MAPE

The phytochemical constituents of MAPE were investigated using LC-DAD/ESI-Ms analysis. One mg MAPE was dissolved in 1 mL in 2 ml methanol/tertiary butyl methyl ether (1: 1, v/v). After membrane filtration (0.45 mm) an aliquot of the solution was subjected to the LC/MS system. The whole procedure was performed in dim light.

LC-DAD/ESI-Ms analysis: An Agilent MSD SL Trap mass spectrometer was connected to an Agilent Technologies Series 1100 HPLC system *via* an ESI interface, composed of an automatic sample injection system, a dual pump, a constant vacuum de-gasser and a column temperature controller (Agilent Technologies, USA). All the operations, the acquiring and analysis of data were controlled by MSD Trap Control Version 4.2 software (Agilent Technologies, USA). The chromatographic analysis was established on a Kromasil RP-C18 (4.6 mm × 150 mm, 5 µm) column at room temperature. The mobile phase was prepared from methanol, *tert*-butyl methyl ether, and water at 81 : 15: 4, v/v/v (A) and 6 : 90: 4, v/v/v (B), starting with 10 min isocratic at 100% A, then by a gradient to obtain 50% B at 40 min, 100% B at 50 min, 100% A at 55 min and isocratic 100% A from 55 min to 60 min at a flow rate of 1 ml/min. All solvents were filtered through a 0.45 µm nylon filter prior to use. The flow rate was adjusted at 1 mL/min. The effluent was split into two parts where one part was injected into MS detector (10 µL) at 0.3 mL/min. Compounds were detected along a range of m/z 50 to 3000 using a MicroTOF-Q hybrid

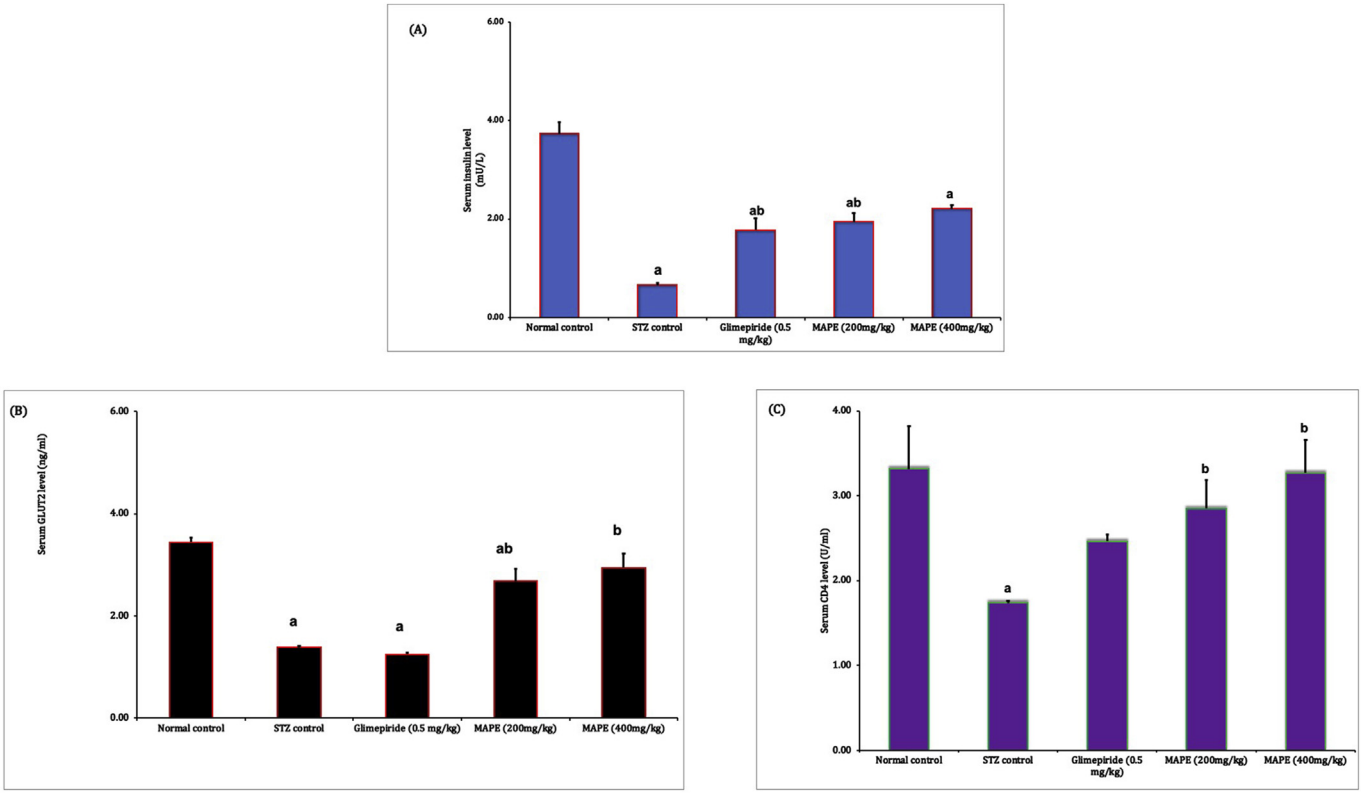

Fig. 3. Effect of MAPE on (A) serum insulin level, (B) serum GLUT 2 level, (C) serum CD4 level; Data were expressed as mean ± SE. Statistical analysis was carried out by one-way ANOVA followed by Tukey HSD test for multiple comparisons. [a] Significantly different from normal control at $P < 0.05$. [b] Significantly different from STZ control at $P < 0.05$.

Table 3
Effect of MAPE on oxidative stress and antioxidant status.

	Normal control	STZ control	Glimepiride (0.5 mg/kg)	MAPE (200 mg/kg)	MAPE (400 mg/kg)
NO (μmol/L)	50.34 ± 0.74	159.16 ± 0.75 [a]	103.45 ± 7.13 [ab]	59.16 ± 3.30 [b]	50.92 ± 0.60 [b]
MDA (nmol/L)	9.70 ± 0.09	50.11 ± 2.36 [a]	9.19 ± 0.21 [b]	9.55 ± 0.07 [b]	8.76 ± 0.42 [b]
Catalase (U/L)	442.22 ± 14.45	182.78 ± 7.04 [a]	233.33 ± 2.72 [ab]	271.11 ± 1.86 [ab]	308.89 ± 4.99 [ab]

Data were expressed as mean ± SE. Statistical analysis was carried out by one-way ANOVA followed by Tukey HSD test for multiple comparisons. [a] Significantly different from normal control at $P < 0.05$. [b] Significantly different from STZ control at $P < 0.05$.

quadrupole time-of-flight mass spectrometer (Bruker Daltonics) with ESI orthogonal electrospray ion source in positive ion mode.

Tandem Mass Spectrometry (MS–MS): Precursor ions were detected and fragmented in the collision cell with Argon being the collision gas and applying collision energies in the range of 10–30 eV. The produced ions were estimated using pulser with 10 kHz frequency and 1.5 Hz spectra rate. MS/MS spectra were detected on Thermo Orbitrap Fusion instrument with Thermo Ultimate 3000 RSLC system and Agilent Zobax-SB C18 column (ThermoElectron, San Jose, USA), using the same elution gradient as in HPLC-MS. The system is equipped with an ESI source (electrospray voltage 4.0 kV, sheath gas: nitrogen; capillary temperature: 275 °C) in positive ionization mode.

Compounds were identified according to their retention times, mass spectra, UV absorbance and comparison to Mass Bank database and reference literature.

3. Results and discussion

3.1. Algal dynamics and predominance in the high rate algal pond

The high rate algal pond operation started in summer months which lead to the predominance of *Microcystis flos aqua*, *Microcystis aureginosa* and other species of *Microcystis*. Always, different *Microcystis* sp. represent the upper most layer, while near the bottom layer of the pond different green and diatoms group are present. Many species include *Scenedesmus obliquus* and *Scenedesmus quadricauda, Ankistrodesmus, Coelosterum microporum, Selenastrum* and *Micractinium pusillum* (green algae group), *Oscillatoria limnetica* (blue green algae group) and *Nitzschia linearis* (diatoms group) was the most present species. Since the beginning of November 2017, the community structure of HRAP completely changed where the *Microcystis* sp. disappeared and the dominance of different algal species took place. In addition, all algal species mixed and floated in pond water column. The predominant algal species are *Scenedesmus obliquus, Scenedesmus quadricauda, Ankistrodesmus, Coelosterum microporum, Selenastrum, Oocystis parva. Dictyosphaerium pulchellum. Coelastrum reticulatum, Pediastrum gracilimum, Siderocells elegans, Eudorina elegans, Clamydomonas reinhardi* and *Micractinium pusillum* (green algae group), *Euglena sp.* (Euglenophyta), *Oscillatoria limnetica* (blue-green algae group) and *Nitzschia linearis* (diatoms group).

During the period of *Microcystis* sp. predominance, algal biomass (from inside the algal pond) were harvested biweekly and precipitated using cationic starch and then dried. The dried algal biomass grinded to fine particles (0.1 mm) and mixed thoroughly.

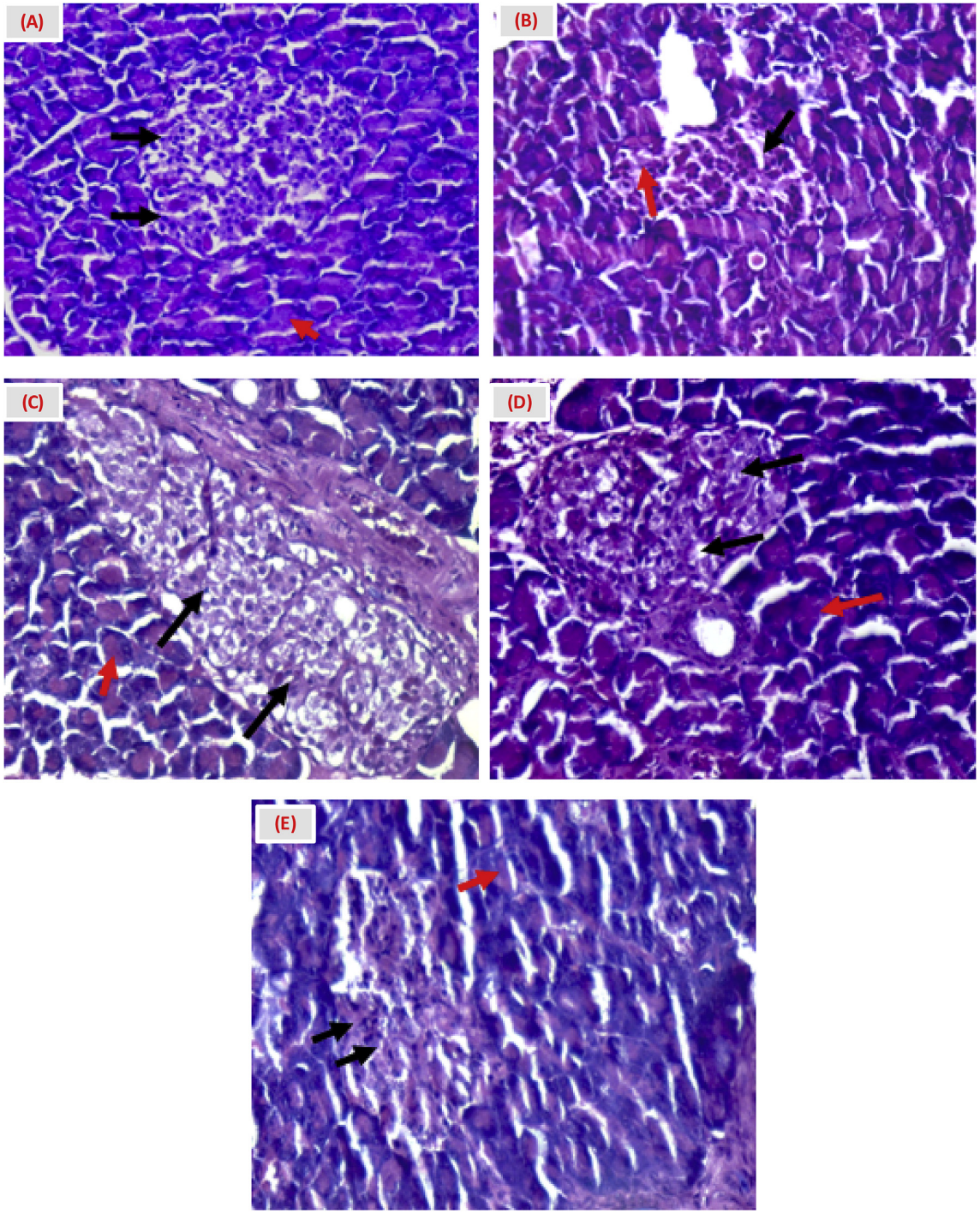

Fig. 4. Pancreatic section from (A) normal control group, (B) STZ group, (C) Glimepiride and (D) rats treated with MAPE (200 mg/kg), (E) rats treated with MAPE (400 mg/kg) (H&E,x400).

3.2. Pharmacological study of MAPE

3.2.1. Acute toxicity study of MAPE

MAPE exhibited no mortality after 24 h of oral administration at graded doses up to a 5 g/kg and according to Semler24 so the determination of an LD50 value was not required. Hence, the chosen experimental dose was 1/10 of 5 g/kg of MAPE (500 mg/kg).

3.2.2. Antioxidant activity (DPPH radical scavenging activity) of MAPE

MAPE at different concentrations of 1250, 2500, 5000, 10000, 20000, 40000 and 80000 µg/ml showed marked antioxidant activity; the scavenging activities were 52.9, 45.5, 42.3, 15.9, 10.1, 4.8 and 3.7%, respectively. The EC_{50} was calculated to be 1.18 mg/ml.

3.2.3. Anti-inflammatory activity of MAPE

3.2.3.1. Effects of pre-treatment with MAPE on Carrageenan induced paw edema. The subplanter injection of 100 µL of 1% sterile carrageenan into the rat hind paw elicited an inflammation (swelling and erythema) and a time-dependent increase in paw edema by 71.57, 92.94, 101.44% and 91.22% at 1st, 2nd 3rd at and 4th hours respectively, as compared with pre-carrageenan control values. Oral administration of MAPE (500 mg/kg) showed a significant inhibition of edema formation at

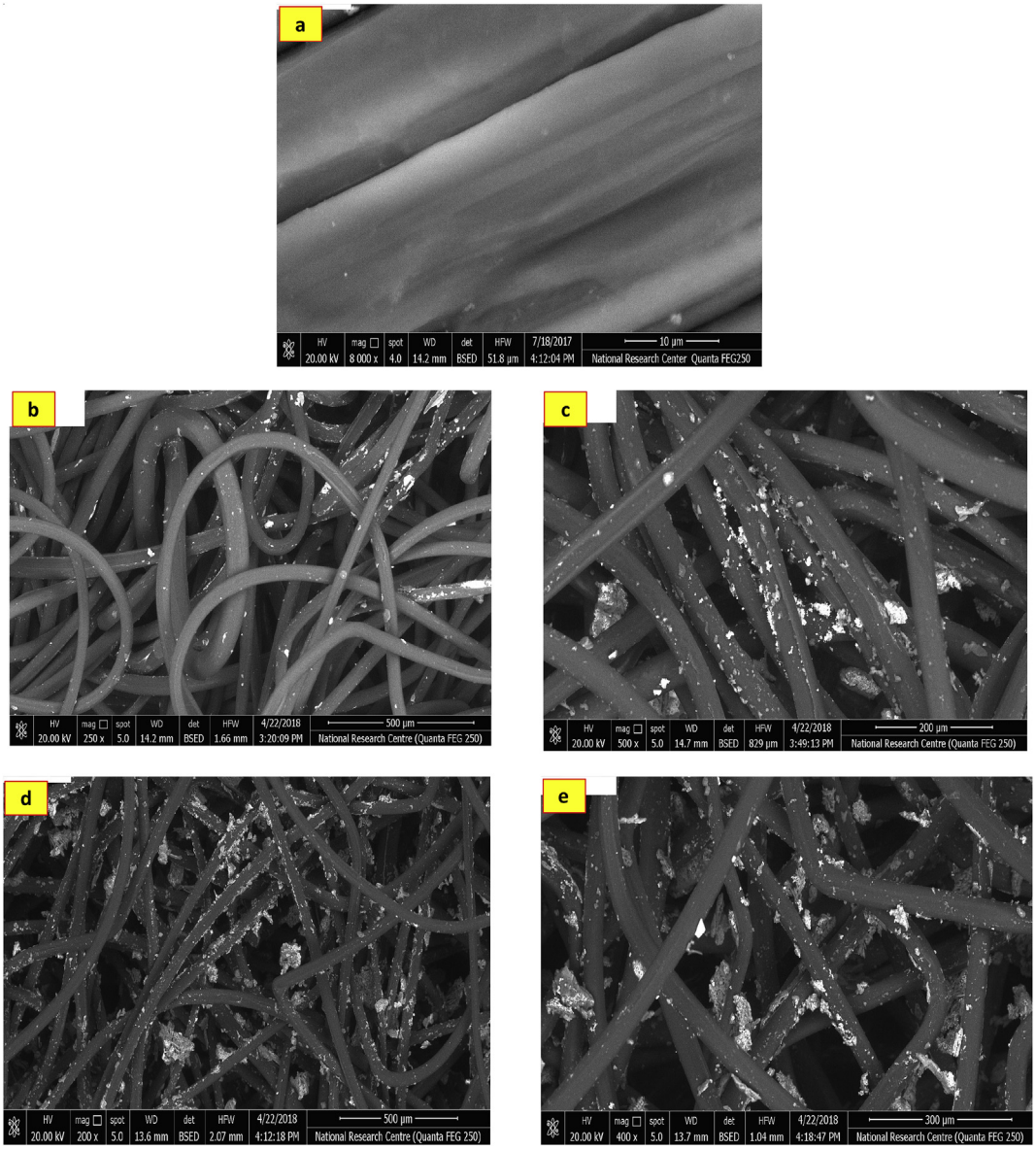

Fig. 5. SEM of (a) untreated cotton bandage fabric, treated cotton bandage fabric with (b,c) 200 mg and (d,e) 400 mg of MAPE.

Table 4
Effects of treatment with MAPE on wound area.

Time	Control	MAPE (200 mg/kg)	MAPE (400 mg/kg)
Zero time	0.74 ± 0.00	0.76 ± 0.01	0.78 ± 0.01
After 7 days	0.68 ± 0.01	0.57 ± 0.00	0.29 ± 0.00

Data were expressed as mean ± SE. Statistical analysis was carried out by one-way ANOVA followed by Tukey HSD test for multiple comparisons. [a] Significantly different from normal control at $P < 0.05$. [b] Significantly different from STZ control at $P < 0.05$.

1st hours by 49.49%, at 2nd hours by 57.39%, at 3rd hours by 59.94% and at 4th hours by 64.51%, as compared with carrageenan control group at the same time point (Table 1). The MAPE has 0.91 indomethacin potency at 4th hours.

3.2.4. Cytotoxic activity of MAPE on human cell lines

MAPE showed potent cytotoxic activity on PC3 prostate cancer cell line with 100% inhibition of cell viability at a dose of 100 ppm. It also showed potent activity on HePG 2 human hepatocellular carcinoma cell line and MCF-7 human caucasian breast adenocarcinoma with 81.1% and 64.3% decrease in cell count, respectively. The cytotoxic effect of the MAPE was limited in the case of lung and colon cancer cell lines. Results are shown in Table 2.

3.2.5. Anti-diabetic assay of MAPE

3.2.5.1. Effect of MAPE on blood glucose level. Blood glucose level of diabetic rats was increased significantly by 5 fold as compared to the control groups. Treatment with MAPE at dose (200 and 400 mg/kg b.wt.) significantly decreased the glucose level of the diabetic groups in dose dependent manner by 56% and 83%, respectively, when compared diabetic control rats. Glimepiride-treatment reduced the blood glucose level by 48% when compared diabetic control rats as illustrated in (Fig. 2).

Table 3 outlined the effect of MAPE on oxidative stress and anti-oxidant status. It was clearly seen that the serum NO and MDA levels of diabetic rats were increased significantly by 216% and 416%, respectively, as compared to the control group. Treatment with MAPE at dose (200 and 400 mg/kg b.wt.) significantly decreased NO serum level of the diabetic groups in dose dependent manner by 63% and 68% and reduced MDA serum level by 81% and 83%, respectively, when

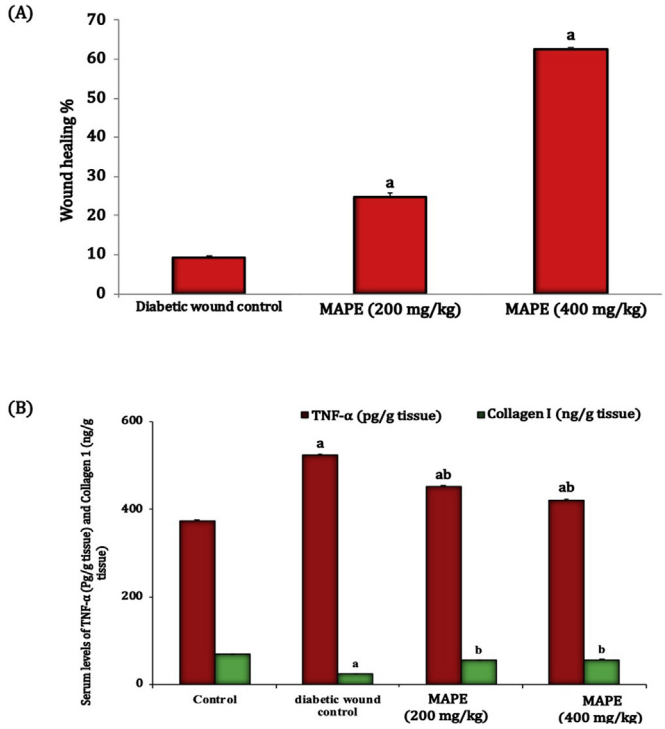

Fig. 6. Effects of treatment with MAPE on (A) wound healing (%) and (B) skin contents of TNF-α and collagen I. Each data point represents mean ± SE (n = 8). [a] significantly different from diabetic wound control at $P < 0.05$. [b] significantly different from diabetic wound control at $P < 0.05$.

compared diabetic control rats.

Glimepiride-treatment reduced NO and MDA serum levels by 35% and 82%, respectively, when compared diabetic control rats (Table 3). Serum catalase level of diabetic rats was decreased significantly by 59%, as compared to the control group. Treatment with MAPE at dose (200 and 400 mg/kg b.wt.) significantly elevated serum catalase level by 48% and 69%, respectively, when compared diabetic control rats. Glimepiride-treatment increased catalase serum level by 28%, when compared diabetic control rats (Table 3).

Fig. 3A showed the effect of MAPE on serum insulin level. It was clearly seen that the serum insulin level of diabetic rats was decreased significantly by 82% as compared to the control group. Treatment with MAPE at dose (200 and 400 mg/kg b.wt.) significantly increased serum insulin level in dose dependent manner by 196% and 236%, respectively, when compared diabetic control rats. Glimepiride-treatment increased serum insulin level by 170% after 1 week when compared diabetic control rats as illustrated in Fig. 3A. Meanwhile the effect of MAPE on serum GLUT2 level was illustrated in Fig. 3B. As shown in Fig. 3B the serum GLUT2 level of diabetic rats was decreased significantly by 60% as compared to the control group. Treatment with MAPE at dose (200 and 400 mg/kg b.wt.) significantly increased serum GLUT2 level in dose dependent manner by 93% and 112%, respectively, when compared diabetic control rats. Glimepiride-treatment did not change serum GLUT2 level when compared diabetic control rats.

Fig. 3C shows the Effect of MAPE on serum CD4 level. It was observed that the serum CD4 level of diabetic rats was reduced significantly by 48% as compared to the control group. Treatment with MAPE at dose (200 and 400 mg/kg b.wt.) siginficantly increased serum CD4 level in dose dependent manner by 64% and 88%, respectively, when compared diabetic control rats. Glimepiride-treatment elevated serum CD4 level by 42% after 1 week when compared diabetic control rats.

3.2.6. Histopathological study of the pancreatic treated rats with MAPE

Pancreatic sections of the untreated and treated rats with MAPE were depicted in Fig. 4. The Pancreatic section from the normal control group (Fig. 4A) showed pancreatic islets were shaped regularly and arranged evenly, with normal islets of Langerhans (black arrows) and normal acini tissues (red arrows). Meanwhile the pancreatic section for STZ group as illustrated in Fig. 4B showed pancreatic islets with irregular islets of Langerhans cells, not well defined (black arrows), necrosis of cells (red arrow). Pancreatic section from Glimepiride as shown in Fig. 4C showed pancreatic islets were shaped regularly and arranged evenly, with normal islets of Langerhans (black arrows) and normal acini tissues (red arrows). Fig. 4D showed the pancreatic section of the rats treated with MAPE (200 mg/kg) showed pancreatic islets were shaped regularly and arranged evenly, with almost normal islets of Langerhans (black arrows) and normal acini tissues (red arrows). On the hand, Fig. 4E present the pancreatic section of the rats treated with MAPE (400 mg/kg) showed pancreatic islets were shaped regularly and arranged evenly, with almost normal islets of Langerhans (black arrows) and normal acini tissues (red arrows) (H&E,x400).

3.3. Morphological structure of untreated and treated cotton bandage fabric with MAPE solution

The target of our work is designed to fabricate cotton bandage fabric treated with eco-friendly materials produced from useless wastes. Thus, the environmentally prepared cotton bandage fabric can be used as disposable item for single application such as surgical bandage or as in our work to use as bandage for diabetic ulcers. The surface morphological features of cotton bandage fabric before and after treatment with the two concentration of MAPE (200 mg and 400 mg) were given in Fig. 5. Fig. 5 (a) shows the surface of untreated cotton bandage fabric while Fig. 5 (b, d) represent the appearance of surface for the cotton bandage fabric after treatment with 200 mg and 400 mg of MAPE respectively. First of all, there are some clear differences in the respective images of untreated and treated cotton bandage fabrics. The images for the treated cotton surface were taken also at high magnification in Fig. 5 (c,e) to clarify the shape of film deposited on the surface.

It is evident from the surface of untreated cotton bandage fabric as shown in Fig. 5 (a) has smooth surface and the fibrils winding up at an angle to the fiber axis. On contrary, the immersed cotton bandage fabrics in the bath containing 200 mg and 400 mg of MAPE, respectively 200 have significant rough surface due to the deposition of extract on the surface of the treated cotton bandage fabric. Furthermore, the treated cotton bandage fabrics have a film like deposited on the surface beside to some of formed large particles. It is clearly observed that the fabric treated with 400 mg has a heavy deposition of MAPE on the fiber surface. Based on the above observations, the treated cotton bandage fabrics were further applied to the wounds of diabetic rats as outlined below.

3.4. Biochemical analysis for the diabetic rats treated with and without bandages loaded with MAPE

3.4.1. Effects of treatment with MAPE on wound healing and on skin contents of TNF-α and collagen I

The positive control group showed non-healed contracted wound. While treatment with MAPE (200 & 400 mg/kg) decreased wound area relative to the wound area at zero time (Table 4) and revealed more contraction compared to the positive control group by 2 fold and 6 fold respectively, At day 7 post-wounding (Fig. 6A).

3.4.2. Effects of treatment with MAPE on skin contents of TNF-α and collagen I

The skin content of TNF-α was significantly high in the wounded tissue of STZ group by 40% as compared to normal control ($P < 0.05$), while TNF-α skin content was significantly low in the wounded tissue

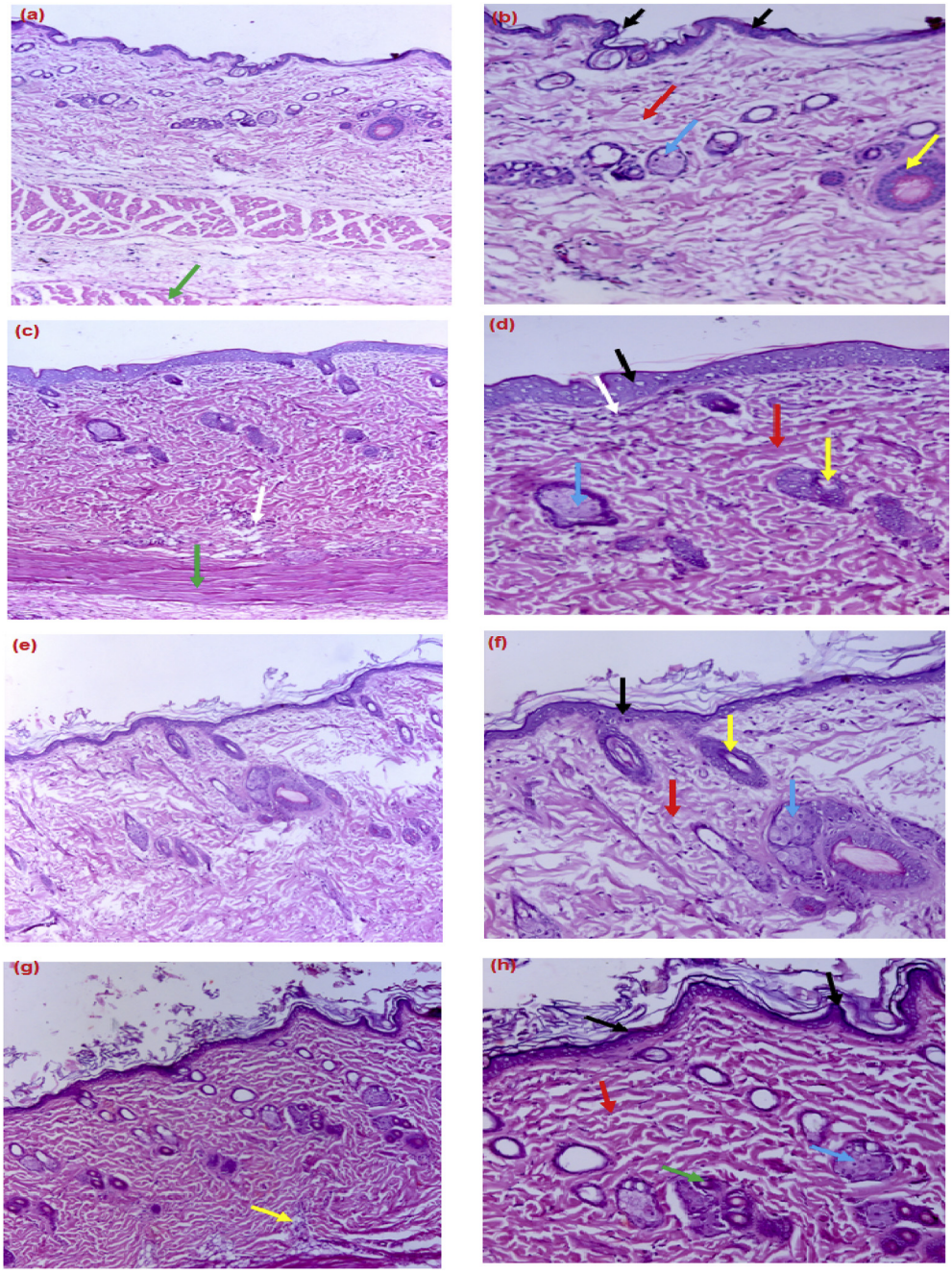

Fig. 7. Histopathological examination for the skin section of (a,b) control group, (c,d) group 1 (treated), (e,f) group 2 (treated) and (g,h) group B (diseased).

treated with both doses of 200 and 400 mg/kg by 14% and 20% respectively, compared to that in the wounded tissue of STZ group. Moreover, the skin content of collagen I was significantly low in the wounded tissue of STZ group by 65% as compared to normal control ($P < 0.05$), while collagen I skin content was significantly high in the wounded tissue treated with both doses of 200 and 400 mg/kg by 127% and 134% respectively, compared to that in the wounded tissue of STZ group (Fig. 6B).

3.5. Histopathological study for the skin sections of untreated rats and rats treated with bandages loaded with different concentrations of MAPE

It is observed form Fig. 7 (a,b) that the skin section from normal control group shows normal skin structure, intact epidermis (external epithelium formed of 2-3 cell layers) (black arrow), dermis (thick layer of connective tissue) (red arrow), a muscle layer (green arrow), sebaceous glands (blue arrow) and intact hair follicles (yellow arrow) (piliary canals)(H&E, x 100, x200). Fig. 7 (c,d) displayed the skin section from group 1 (treated) showed mild hyperplasia of epidermis, intact epidermis (external epithelium more than 2–3 cell layers) (black arrow), dermis (thick layer of connective tissue) (red arrow) and with mild infiltration of lymphocytes and polymorphoneutrophils (white arrow) a muscle layer (green arrow), sebaceous glands (blue arrow) and intact hair follicles (yellow arrow) (piliarycanals). While, Fig. 7 (e,f) represented the skin section from group 2 (treated) which demonstrated that the appearance of normal skin structure, intact epidermis (external epithelium formed of 2-3 cell layers) (black arrow), dermis (thick layer of connective tissue) (red arrow), sebaceous glands (blue arrow) and intact hair follicles (yellow arrow) (piliarycanals). Finally, a mild hyperplasia of epidermis (external epithelium formed of more than 3 cell

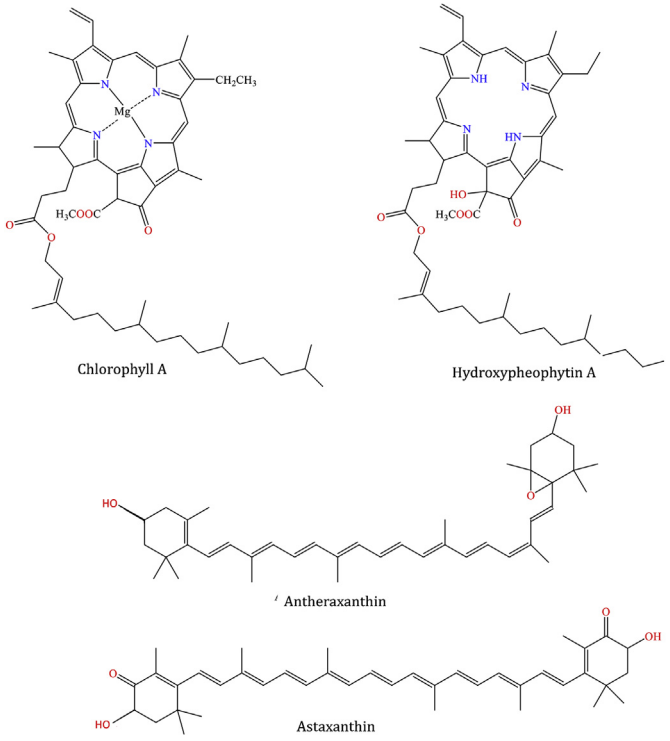

Fig. 8. Chemical structures of identified compounds.

layers) (black arrow), dermis (thick layer of connective tissue) (red arrow) and with mild infiltration of lymphocytes and polymorphoneutrophils (red arrow), sebaceous glands (blue arrow), fat (green arrow) as shown in Fig. 7 (g,h) (H&E, x 100,x200).

Our results demonstrated that MAPE at different concentrations exhibited marked DPPH scavenging activities, moreover; the oral administration of MAPE reversed the edema formation induced by carrageenan at all time points, as compared with carrageenan control group. These results are in a line with previous studies using other different microalgae that have antioxidant and anti-inflammatory effects (Talero et al., 2015).

Many microalgae strains, such as *Aphanizomenon flos-aquae, Chlorella*, and *Arthrospira*, contain high protein content and other health-supporting substances so cultured at a commercial scale (Soletto et al., 2005). These substances reportedly have important pharmacological actions, such as anti-hyperglycemia and anti-hyperlipidemia, which are helpful in diabetes and obesity control because they affect the elevated serum glucose level. In this study, treatment with two dose levels of MAPE (200 & 400 mg/kg) reduced the glucose level of the diabetic rats in dose dependent manner when compared to STZ diabetic control rats and Glimepiride-treated rats. Our results supported by previous study that showed that microalga *Spirulina* exhibited hypoglycemic and hypolipidemic properties in diabetic rats (Joventino et al., 2012).

Carotenoids, phenolic compounds, polysaccharides phycobiliprotein pigments and unsaturated fatty acids, natural algal products, have variable biological activities, such as antioxidant activity, anticancer activity, antimicrobial activity (Shalaby, 2011). In current work, STZ injection elevated serum NO and MDA levels and reduced catalase serum level in diabetic rats, as compared to the normal control group. While, treatment with both doses of MAPE decreased NO and MDA serum levels and elevated serum catalase level of the diabetic groups, when compared to diabetic control rats. In addition MAPE high dose is more potent as antioxidant than Glimepiride. *Dunaliella salina* another microalga reduced MDA and NO levels in diabetic rats (Aly and Ali, 2016).

In the present study, STZ injection decreased serum insulin level of diabetic rats as compared to the control group. Treatment with both doses of MAPE increased serum insulin level, when compared diabetic control rats. Both doses of MAPE restored insulin level more than Glimepiride-treatment and this is explained by our histopathological study that showed normal islets of Langerhans in group treated with MAPE. Ebrahimi-Mameghani found that *Chlorella vulgaris* microalgae increased insulin level in patients suffering from non-alcoholic fatty liver disease (Ebrahimi-Mameghani et al., 2017). In addition, Serum GLUT2 level of diabetic rats was decreased as related to the normal control group. Treatment with both doses of MAPE increased serum GLUT2 level, when compared to diabetic control rats while treatment with Glimepiride did not change serum GLUT2 level when compared diabetic control rats. These results are explained as the diabetes is associated with an intense reduction in the expression of glucose GLUT2 (Joventino et al., 2012). This functional deficit led to under expression of GLUT2 that is a reason of cell insensitivity to glucose and linked with inability to correct hyperglycemia (Unger, 1991). In addition, STZ is toxic glucose analogs that target pancreatic β-cells through GLUT2 transporter uptake (Muller et al., 2011). This fact is supported by our histopathological study that showed irregular islets of Langerhans cells, not well defined associated with necrosis of the cells.

Diabetes induced suppression of regulatory T cells as CD4 cells that have protective activity against autoimmune diseases as gastritis and diabetes (Stephens and Mason, 2000). The current results showed that STZ injection reduced serum CD4 level of diabetic rats relative to the control group. Treatment with both doses of MAPE increased serum CD4 level, when compared diabetic control rats and Glimepiride-treated rats.

Table 5
Compounds identified in the bioactive extract of MAPE, their retention time, molecular weights, UV-absorbances and their relative abundance in the extract.

Peak no.	Retention time	*m/z*	λ_{max} observed	λ_{max} reported	Identification	% of TIC	% of TAC
1	1.47	551.82	475	470	Echinenone	0.37%	0.85%
2	1.72	545.57	277	278	Phytoene	5.94%	-
3	1.88	887.30	400, 665	406, 666	Hydroxypheophytin A	27.17%	21.84%
4	2.074	585.30	280, 395	290, 385	Antheraxanthin	4.60%	5.38%
5	2.128	569.49	420	423, 450, 474	All trans zeaxanthin	-	< 1%
6	2.301	893.52	400, 665	428, 663	Chlorophyll A	-	27.14%
7	2.382	834.54	470	478	Astaxanthin-H-C16:0	7.64%	-
8	2.72	868.672	480	480, 510	4-Ketomyxoxanthophyll	3.73%	13.97%
9	3.04	639.280	470	446, 412, 502	Myxoxanthophyll	2.33%	4.04%
10	3.35	874.783	478	478	Astaxanthin + H-C 20:4	1.43%	1.48%
11	3.82	915.701	410, 665	430, 664	Chlorophyll a-Na^+	1.63%	1.96%
12	12.421	909.3 M + 1	435, 615, 665	422, 614, 660	Hydroxychlorophyll A	-	< 1%
13	14.412	544.42	380		Phytofluene	-	< 1%
14	21.67	653.679	480	429, 449, 477	2,3-Dihydroxy-β-carotene	0.43%	< 1%

Where TIC: Total ion chromatogram, TAC: Total absorbance chromatogram, C16: palmitic acid = D m/z 256 and C20:4 eicosatetraenoic acid = D m/z 276.

3.6. Phytochemical analysis of MAPE

The LC-DAD/ESI-Ms analysis of the bioactive extract of *Microcystis aerigunosa* resulted in the separation and identification of 14 compounds the major of which was chlorophyll a (27.14%) followed by hydroxypheophytin A (magnesium-free chlorophyll A) (21.84%) in addition to a number of carotenoids (astaxanthin, antheraxanthin, 2,3-dihydroxy-β-carotene, echinenone and zeaxanthin), myxoxanthophyll and its keto-derivative (Fig. 8). The identified compounds, their retention times, molecular weights, UV-absorbances and their relative abundance in the extract are presented in Table 5.

The chlorophyll A and pheophytin A (magnesium-free chlorophyll A) were previously shown to exert anti-inflammatory activity against carrageenan-induced inflammation, presumably through inhibition of TNF-α gene expression as well as *in vitro* anti-oxidant activity (Subramoniam et al., 2012). Carotenoids are wide range of pharmacological activities based on their potent antioxidant effect as evidenced by a large scientific body (Krinsky, 2001).

4. Conclusion

The extract of microalgae harvested from high rate algal pond highly predominated by *M. aeruginosa* (MAPE) showed promising pharmacological activities; antioxidant, anti-inflammatory, cytotoxic and antidiabetic activities. Additionally, MAPE based medicated cotton bandages showed marked healing aid activity in diabetic wounds induced in rats. The pharmacological activity is mediated through the high contents of chlorophyll A and hydroxypheophytin A along with the high content of carotenoids. Algal communities growing in high rate algal ponds may satisfy the growing demand for safe and economic pharmaceutical products.

References

Aebi, H., 1984. Catalase in vitro. Methods Enzymol. 105, 121–126.

Aly, H.H., Ali, G., 2016. Antidiabetic efficacy of dunaliella salina extract in stz-induced diabetic. Int. J. Pharma Bio Sci. 7 (3), 0–9.

Arashiro, L.T., Ferrer, I., Rousseau, D.P.L., Van Hulle, S.W.H., Garfí, M., 2019. The effect of primary treatment of wastewater in high rate algal pond systems: biomass and bioenergy recovery. Bioresour. Technol. 280, 27–36. https://doi.org/10.1016/J.BIORTECH.2019.01.096.

Asfour, M.H., Elmotasem, H., Mostafa, D.M., Salama, A.A.A., 2017. Chitosan based Pickering emulsion as a promising approach for topical application of rutin in a solubilized form intended for wound healing: in vitro and in vivo study. Int. J. Pharm. 534, 325–338. https://doi.org/10.1016/J.IJPHARM.2017.10.044.

Assunção, J., Guedes, A.C., Malcata, F.X., 2017. Biotechnological and pharmacological applications of biotoxins and other bioactive molecules from dinoflagellates. Mar. Drugs 15. https://doi.org/10.3390/md15120393.

Bilal, M., Rasheed, T., Sosa-Hernández, J., Raza, A., Nabeel, F., Iqbal, H., Bilal, M., Rasheed, T., Sosa-Hernández, J.E., Raza, A., Nabeel, F., Iqbal, H.M.N., 2018. Biosorption: an interplay between marine algae and potentially toxic elements—a review. Mar. Drugs 16, 65. https://doi.org/10.3390/md16020065.

Craggs, R.J., Heubeck, S., Lundquist, T.J., Benemann, J.R., 2011. Algal biofuels from wastewater treatment high rate algal ponds. Water Sci. Technol. 63, 660–665. https://doi.org/10.2166/wst.2011.100.

Desoukey, S.Y., Kady, W.M. El, Salama, A.A.A., Hagag, E.G., Siham, M., 2016. Hepatoprotection and antioxidant activity of gazania longiscapa and G . Rigens with the isolation and quantitative analysis of bioactive metabolites. Int. J. Pharmacogn. Phytochem. Res 8, 1121–1131.

Ebrahimi-Mameghani, M., Sadeghi, Z., Abbasalizad Farhangi, M., Vaghef-Mehrabany, E., Aliashrafi, S., 2017. Glucose homeostasis, insulin resistance and inflammatory biomarkers in patients with non-alcoholic fatty liver disease: beneficial effects of supplementation with microalgae Chlorella vulgaris : a double-blind placebo-controlled randomized clinical trial. Clin. Nutr. 36, 1001–1006. https://doi.org/10.1016/j.clnu.2016.07.004.

El-Baz, F., Abdel Jaleel, G., Saleh, D., Hussein, R., 2018. Protective and therapeutic potentials of Dunaliella salina on aging-associated cardiac dysfunction in rats. Asian Pac. J. Trop. Biomed. 8, 403. https://doi.org/10.4103/2221-1691.239428.

El-Naggar, M.E., Al-Joufi, F., Anwar, M., El-Bana, M.A., Attia, M.F., et al., 2019. Curcumin-loaded PLA-PEG copolymer nanoparticles for treatment of liver inflammation in streptozotocin-induced diabetic rats. Colloids and Surfaces B: Biointerfaces 177, 389–398.

El-Naggar, M.E., Samhan, F.A., Salama, A.A.A., Hamdy, R.M., Ali, G.H., 2018. Cationic starch: safe and economic harvesting flocculant for microalgal biomass and inhibiting E. coli growth. Int. J. Biol. Macromol. 116, 1296–1303. https://doi.org/10.1016/j.ijbiomac.2018.05.105.

El-Naggar, M.E., Shaarawy, S., Hebeish, A., 2018. Multifunctional properties of cotton fabrics coated with in situ synthesis of zinc oxide nanoparticles capped with date seed extract, C. arbohydrate polymers 181, 307–316.

Elshaarawy, R.F., El-Naggar, M.E., Mostafa, T.B., El-sawi, E.A., Seif, G.A., 2019. In-situ and ex-situ synthesis of poly-(imidazolium vanillyl)-grafted chitosan/silver nanobiocomposites for safe antibacterial finishing of cotton fabrics. European Polymer Journal 116, 210–221.

Fehrenbacher, J.C., Vasko, M.R., Duarte, D.B., 2012. Models of inflammation: carrageenan- or complete Freund's Adjuvant (CFA)-induced edema and hypersensitivity in the rat. Curr. Protoc. Pharmacol (Chapter 5), Unit5.4. https://doi.org/10.1002/0471141755.ph0504s56.

Gross, M., Jarboe, D., Wen, Z., 2015. Biofilm-based algal cultivation systems. Appl. Microbiol. Biotechnol. 99, 5781–5789. https://doi.org/10.1007/s00253-015-6736-5.

HAYASHI, K., HAYASHI, T., KOJIMA, I., 1996. A natural sulfated polysaccharide, calcium spirulan, isolated from *Spirulina platensis: in vitro* and *ex vivo* evaluation of anti-herpes simplex virus and anti-human immunodeficiency virus activities. AIDS Res. Hum. Retrovir. 12, 1463–1471. https://doi.org/10.1089/aid.1996.12.1463.

Hussein, J., El-Banna, M., Razik, T.A., El-Naggar, M.E., 2018. Biocompatible zinc oxide nanocrystals stabilized via hydroxyethyl cellulose for mitigation of diabetic complications. International journal of biological macromolecules 107, 748–754.

Joventino, I.P., Alves, H.G.R., Neves, L.C., Pinheiro-Joventino, F., Leal, L.K.A.M., Neves, S.A., Ferreira, F.V., Brito, G.A.C., Viana, G.B., 2012. The microalga Spirulina platensis presents anti-inflammatory action as well as hypoglycemic and hypolipidemic properties in diabetic rats. J. Complement. Integr. Med. 9 Article 17. https://doi.org/10.1515/1553-3840.1534.

Khalaf, M.M.A., Sherbiny, G.A., Abdellatif, H.A., 2012. Comparative effects of glimepiride , vanadyl sulfate and their combination on hypoglycemic parameters and oxidative stress. Br. J.Pharmacol. Toxicol. 3, 278–288.

Krinsky, N.I., 2001. Carotenoids as antioxidants. Nutrition 17, 815–817. https://doi.org/10.1016/S0899-9007(01)00651-7.

Mazur-Marzec, H., Fidor, A., Cegłowska, M., Wieczerzak, E., Kropidłowska, M., Goua, M., Macaskill, J., Edwards, C., 2018. Cyanopeptolins with trypsin and chymotrypsin inhibitory activity from the cyanobacterium nostoc edaphicum CCNP1411. Mar. Drugs 16. https://doi.org/10.3390/md16070220.

Mihara, M., Uchiyama, M., 1978. Determination of malonaldehyde precursor in tissues by thiobarbituric acid test. Anal. Biochem. 86, 271–278.

Miranda, K.M., Espey, M.G., Wink, D.A., 2001. A rapid, simple spectrophotometric method for simultaneous detection of nitrate and nitrite. Nitric Oxide 5, 62–71. https://doi.org/10.1006/niox.2000.0319.

Moron, M.S., Depierre, J.W., Mannervik, B., 1979. Levels of glutathione, glutathione reductase and glutathione S-transferase activities in rat lung and liver. Biochim. Biophys. Acta 582, 67–78.

Muller, Y.D., Golshayan, D., Ehirchiou, D., Wyss, J.C., Giovannoni, L., Meier, R., Serre-Beinier, V., Puga Yung, G., Morel, P., Bühler, L.H., Seebach, J.D., 2011. Immunosuppressive effects of streptozotocin-induced diabetes result in absolute lymphopenia and a relative increase of T regulatory cells. Diabetes 60, 2331–2340. https://doi.org/10.2337/db11-0159.

Murakami, M., Ishida, K., Okino, T., Okita, Y., Matsuda, H., Yamaguchi, K., 1995. Aeruginosins 98-A and B, trypsin inhibitors from the blue-green alga Microcystis aeruginosa (NIES-98). Tetrahedron Lett. 36, 2785–2788. https://doi.org/10.1016/0040-4039(95)00396-T.

Obukowicz, M.G., Welsch, D.J., Salsgiver, W.J., Martin-Berger, C.L., Chinn, K.S., Duffin, K.L., Raz, A., Needleman, P., 1998. Novel, selective delta 6 or delta 5 fatty acid desaturase inhibitors as antiinflammatory agents in mice. J. Pharmacol. Exp. Ther. 287, 157–166.

Oswald, W., Gotass, H., 1957. Photosynthesis in sewage treatment. Trans. Am. Soc. Civ. Eng (United States) 122.

Posadas, E., García-Encina, P.-A., Soltau, A., Domínguez, A., Díaz, I., Muñoz, R., 2013. Carbon and nutrient removal from centrates and domestic wastewater using algal–bacterial biofilm bioreactors. Bioresour. Technol. 139, 50–58. https://doi.org/10.1016/J.BIORTECH.2013.04.008.

Salama, A.A.A., Yassen, N.N., 2017. CODEN (USA): PCHHAX a cytoprotectant effect of morus alba against streptozotocin-induced diabetic damage in rat brains. Der Pharma Chem. 9, 24–30.

Shalaby, E.A., 2011. Algae as promising organisms for environment and health. Plant Signal. Behav. 6, 1338–1350.

Singh, B., Liu, Y., Sharma, Y.C., 2013. Synthesis of biodiesel/bio-oil from microalgae. In: Biotechnological Applications of Microalgae: Biodiesel and Value-Added Products, pp. 99–112. https://doi.org/10.1201/b14920.

Soletto, D., Binaghi, L., Lodi, A., Carvalho, J.C.M., Converti, A., 2005. Batch and fed-batch cultivations of Spirulina platensis using ammonium sulphate and urea as nitrogen sources. Aquaculture 243, 217–224. https://doi.org/10.1016/J.AQUACULTURE.2004.10.005.

Stephens, L.A., Mason, D., 2000. CD25 is a marker for CD4+ thymocytes that prevent autoimmune diabetes in rats, but peripheral T cells with this function are found in both CD25+ and CD25- subpopulations. J. Immunol. 165, 3105–3110.

Streble, H., Krauter, D., 2006. Das Leben im Wassertropfen: Mikroflora und Mikrofauna des Süsswassers. Ein Bestimmungsbuch. Ein Bestimmungsbucn mit 1700Abbildungen stultart.

Subramoniam, A., Asha, V.V., Nair, S.A., Sasidharan, S.P., Sureshkumar, P.K., Rajendran, K.N., Karunagaran, D., Ramalingam, K., 2012. Chlorophyll revisited: anti-inflammatory activities of chlorophyll a and inhibition of expression of TNF-α gene by the same. Inflammation 35, 959–966. https://doi.org/10.1007/s10753-011-9399-0.

Talero, E., García-Mauriño, S., Ávila-Román, J., Rodríguez-Luna, A., Alcaide, A., Motilva, V., 2015. Bioactive compounds isolated from microalgae in chronic inflammation and cancer. Mar. Drugs 13, 6152–6209. https://doi.org/10.3390/md13106152.

Tsai, C.-C., Emau, P., Jiang, Y., B Agy, M., Shattock, R., Schmidt, A., Morton, W., Gustafson, K., R Boyd, M., 2004. Cyanovirin-N Inhibits AIDS Virus Infections in Vaginal Transmission Models, AIDS Research and Human Retroviruses. https://doi.org/10.1089/088922204322749459.

Unger, R.H., 1991. Diabetic hyperglycemia: link to impaired glucose transport in pancreatic beta cells. Science 251, 1200–1205.